Supplementary Information

Table S1: COMSOL reactions and kinetic rate constants

#	Reaction	Rate Constant	Rate Constant Value	Reference
1	$E + hv \rightarrow E_s$		$R_i = \frac{I_0}{bE'}\left(1 - 10^{-\varepsilon C_E b}\right)$	Beer-Lambert Law
2	$E_s \rightarrow E$	k_{ic}	1.2E8 s^{-1}	[1]
3	$E_s \rightarrow E_t$	k_{isc}	5.0E8 s^{-1}	[1]
4	$E_s \rightarrow E + hv$	k_f	2.0E8 s^{-1}	[1]
5	$E_s + TEOA \rightarrow E + TEOA$	k_q	3.4E9 s^{-1}	[1]
6	$E_t \rightarrow E$	k_{deact}	5.4E2 s^{-1}	[2]
7	$E_t + E \rightarrow 2E$	k_{te}	3.0E8 L/mol·s	[2]
8	$E_t + TEOA \rightarrow E^{\cdot} + TEOA^{\cdot +}$	k_i	4.2E7 L/mol·s	[1]
9	$TEOA^{\cdot +} + OH^- \rightarrow TEOA^{\cdot} + H_2O$	k_{TEArad}	1.0E10 L/mol·s	[3]
10	$TEOA^{\cdot} + O_2 \rightarrow TEOA^+ + O_2^{\cdot -}$	k_{TEA-O2}	3.5E9 L/mol·s	[3]
11	$TEOA^{\cdot} + PEDGA \rightarrow P_n^{\cdot}$	k_{pA}	2.17E4 L/mol·s	[4]
12	$TEOA^{\cdot} + VP \rightarrow P_n^{\cdot}$	k_{pB}	7.66E4 L/mol·s	[5]
13	$P_n^{\cdot} + PEDGA \rightarrow P_{n+1}^{\cdot}$	k_{pA}	2.17E4 L/mol·s	[4]
14	$P_n^{\cdot} + VP \rightarrow P_{n+1}^{\cdot}$	k_{pB}	7.66E4 L/mol·s	[5]
15	$E^{\cdot} + H^+ \rightarrow EH^{\cdot}$	k_{ab}	4.0E9 L/mol·s	[6]
16	$EH^{\cdot} + OH^- \rightarrow E^{\cdot} + H_2O$	k_{af}	2.0E10 L/mol·s	[6]
17	$E^{\cdot} + O_2 \rightarrow E + O_2^{\cdot -}$	k_{regen}	1.0E9 L/mol·s	[7]
18	$TEOA^{\cdot} + EH^{\cdot} \rightarrow E + TEOA$	k_{regen2}	1.0E8 L/mol·s	*
19	$EH^{\cdot} + EH^{\cdot} \rightarrow E + EH_2$	k_{leuco}	4.2E6 L/mol·s	[8]
20	$P_n^{\cdot} + TEOA^{\cdot} \rightarrow P_{n+1}$	k_t	7.55E5 L/mol·s	[9]
21	$P_n^{\cdot} + P_n^{\cdot} \rightarrow P_{n+n}$	k_t	7.55E5 L/mol·s	[9]
22	$P_n^{\cdot} + O_2 \rightarrow P_nOO^{\cdot}$	k_{inh}	4.9E9 L/mol·s	[10]

*assumed to match eosin conc vs. time curve

Table S2: Diffusion constant values

Diffusion Constant	Value (m^2/s)	Diffusion Species
D_E	5.500E-10	Eosin Y
D_{Es}	5.500E-10	Eosin Y (singlet excited)
D_{Et}	5.500E-10	Eosin Y (triplet excited)
D_{E*}	5.500E-10	Eosin Y radical trianion
D_{EH*}	5.500E-10	Protonated Eosin Radical
D_{EH2}	5.500E-10	Leuco Eosin Y
D_{TEOA}	7.043E-10	Treithanolamine
D_{TEOA*+}	7.043E-10	Triethanolamine radical cation

D_{TEOA*}	7.043E-10	Triethanolamine radical
D_{TEOA+}	7.043E-10	Triethanolamine cation
D_{O2}	1.960E-9	Oxygen
D_{OO-}	1.960E-9	Superoxide
D_{PEGDA}	9.013E-10	Polyethylene glycol diacrylate
D_{VP}	9.013E-10	Vinyl pyrrolidinone
D_{Pn*}	9.013E-10	Polymer chain radical (n-units long)
D_{Pn}	9.013E-10	Polymer (n-units long)
D_{PnOO*}	9.013E-10	Peroxy radical

Table S3: COMSOL variable values

Variable	Initial Value	Description
C_E	0.6 µM	Eosin Y concentration
C_{Es}	0	Eosin Y (singlet) concentration
C_{Et}	0	Eosin Y (triplet) concentration
C_{E*}	0	Eosin Y radical concentration
C_{EH*}	0	Protonated eosin radical concentration
C_{EH2}	0	Leuco eosin Y concentration
C_{TEOA}	150 mM	Treithanolamine concentration
C_{TEOA*+}	0	Triethanolamine radical cation concentration
C_{TEOA*}	0	Triethanolamine radical concentration
C_{TEOA+}	0	Triethanolamine cation concentration
C_{O2}	0.58 mM	Oxygen concentration
C_{OO-}	0	Superoxide concentration
C_{PEGDA}	200 mM	Polyethylene glycol diacrylate concentration
C_{VP}	100 mM	Vinyl pyrrolidinone concentration
C_{Pn*}	0	Polymer chain radical (n-units long) concentration
C_{Pn}	0	Polymer (n-units long) concentration
C_{PnOO*}	0	Peroxy radical concentration
C_{H+}	1.26 mM	Proton concentration
C_{OH-}	7.94 mM	Hydroxide ion concentration
I_0	250 W/m^2	Light Intensity
ε	85800 L/(mol*cm)	Extinction coefficient eosin Y (0-1µM)
b	0.39 mm	Light path length through droplet
E'	2.39 J/mol	Energy of photons at 500 nm
δ	0.1 mm	Oxygen boundary layer in water

Materials

Whatman Grade 1 chromatography paper was purchased from VWR (Radnor, PA, USA). Poly(ethylene glycol) diacrylate (Mn=575) (PEGDA), triethanolamine (TEOA), 1-vinyl-2-pyrrolidinone (VP), eosin Y disodium salt, dimethyl sulfoxide (DMSO), 10X phosphate buffered saline (PBS), phenolphthalein, hydrogen chloride, and Tween® 20 were obtained from Sigma Aldrich (St. Louis, MO, USA). Eosin-5-isothiocyanate (EITC) was obtained from Marker Gene Technology (Eugene, OR, USA). Streptavidin was obtained from Rockland Immunochemicals Inc. UltraCruzTM Micro G-25 Spin Columns were purchased from Santa Cruz Biotechnology Inc. (Santa Cruz, CA, USA). CBD-fused, SA-binding variant of reduced charge protein Sso7d from Sulfolobus solfataricus was expressed and purified by Eric A. Miller as described previously[11].

Conjugation of eosin to streptavidin

The method of conjugation of EITC to proteins has been described previously[12,13]. EITC (1 mg) was dissolved in 100 µL of DMSO to prepare a 10 mg/mL EITC stock solution. To prepare the streptavidin conjugate, 10 µL of the EITC stock solution was mixed with a 100 µL solution of streptavidin (1 mg/mL) in 0.1 M sodium bicarbonate buffer (pH 9.7) to give a total reaction volume of 110 µL and the reaction mixture was protected from light and placed at 4 °C overnight. During the reactions, the isothiocyanate functional group of EITC reacts with the amine group of the lysine residues of the proteins to form a thiourea bond. At the end of the reaction, the excess EITC was separated from the eosin-conjugated streptavidin by size-exclusion chromatography with Sephadex matrix (Micro G-25 Spin-Column). UV–visible absorbance spectroscopy was used to determine the concentration of the protein and the average number of eosin molecules coupled to each streptavidin molecule by taking an absorbance scan of the purified conjugate, and using the following equation.

$$\frac{n_{EITC}}{n_{SA}} = \left(Abs_{525}/\varepsilon_{EITC,\,525}\right)/\left[\left\{Abs_{280} - \left(Abs_{525}\varepsilon_{EITC,280}/\varepsilon_{EITC,\,525}\right)\right\}/\varepsilon_{SA,\,280}\right]$$

Where n_{EITC} is the number of molecules of eosin, n_{SA} is the number of molecules of streptavidin, Abs_{280} and Abs_{525} are the measured absorbance values at 280 nm and 525 nm, respectively, $\varepsilon_{EITC,280}$ is 26,800 $M^{-1}cm^{-1}$, $\varepsilon_{SA,280}$ is 173,000 $M^{-1}cm^{-1}$, and $\varepsilon_{EITC,525}$ is 90,200 $M^{-1}cm^{-1}$.
The purified and characterized conjugates were diluted to make 50% v/v glycerol stock and stored at -20 °C until use.

Sensitivity Analysis of Parameters Estimated from Literature

While many system-specific variables were measured directly, kinetic rate constants and oxygen boundary layer thickness were estimated from similar systems in literature. Therefore, we performed a sensitivity analysis on oxygen boundary layer thickness and key kinetic parameters to observe the effects on $t_{0.2}$ if estimated parameter values were increased by 10%. Literature values for k_{ic}, k_{isc}, and k_f were obtained in water at neutral-to-high pH, which is quite different from our system. Therefore these rate constants, as well as $k_{TEA\text{-}O2}$, k_{regen}, and k_{inh}—which are associated with key oxygen inhibition reactions—were chosen for the sensitivity analysis. Oxygen boundary layer, which was estimated from literature[14], was also included.

Only minor changes in $t_{0.2}$ were observed in most parameters, but rate constants associated with generation of triplet eosin (k_{ic}, k_{isc}, and k_f) did demonstrate more sensitivity to perturbation, with k_{isc}, the rate constant associated with reaction of excited singlet eosin Y to excited triplet eosin Y, showing the most significant change (-5.2%). Given that triplet eosin is critical for eosin radical formation and subsequent overcoming of oxygen inhibition and polymerization, this sensitivity makes sense. Oxygen boundary layer demonstrated some sensitivity as well, which was expected, given its key role in determining flux of oxygen into the reaction volume. It is likely that measurement of these values for this specific system could increase the accuracy of the model if needed.

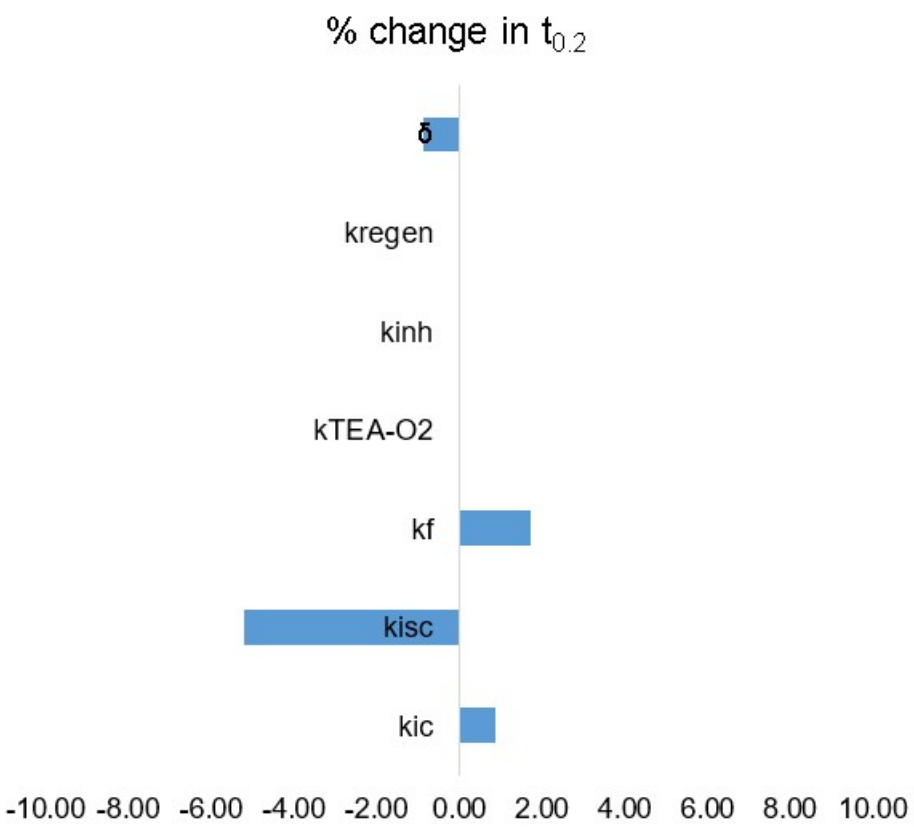

Figure S1: Sensitivity of gelation time ($t_{0.2}$) to 10% perturbations in estimated kinetic rate constants and oxygen boundary layer

Streptavidin-eosin biodetection assay fluorescence results

For all biodetection assays (capture of eosin-conjugated streptavidin by paper-immobilized streptavidin binders), the surface concentration of captured eosin was kept constant for all well sizes to fairly compare eosin photopolymerization signal amplification response across different well sizes and with different monomer solution droplet volumes. Eosin's fluorescence properties were used to assess paper-based streptavidin-eosin capture and compare between replicates and between well sizes.

Fluorescence images to detect surface-immobilized eosin species were acquired using an Olympus IX-81 microscope with a Texas Red filter set (Ex. 560/55, Em. 645/75). Fluorescence intensity measurements were conducted in Image J.

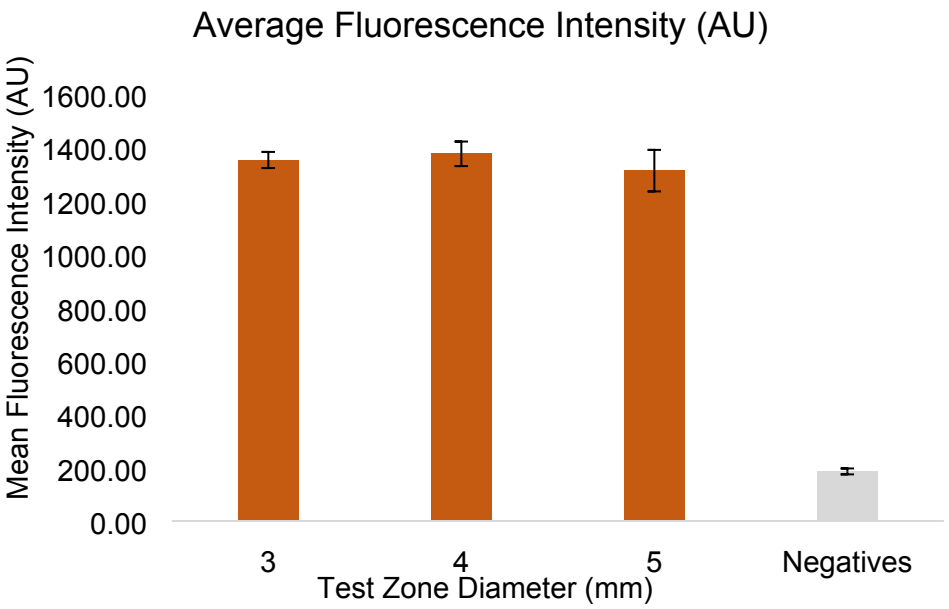

Figure S2: Mean fluorescence intensity of test zones of varied diameter. Negative tests had no streptavidin binder immobilized on the surface. All tests were contacted with streptavidin-eosin. Each bar represents 9 replicates.

Model-predicted and experimental conversion for shallower droplets

Extensive exposure of the reaction volume to oxygen (here, in the form of increased droplet surface area-to-volume ratio) will, at a certain point, prevent any polymerization from occurring. While polymer will form in 3 mm and 5 mm diameter test zones when 20 µL droplets of monomer solution are applied (Figure 4B), both the model and experimental results demonstrated that 3 µL and 10 µL droplets on 3 and 5 mm test zones, respectively, will never form visible polymer, even after 200 s of irradiation with green light. Free eosin Y concentration was set to 0.4 uM for both the model and experiment.

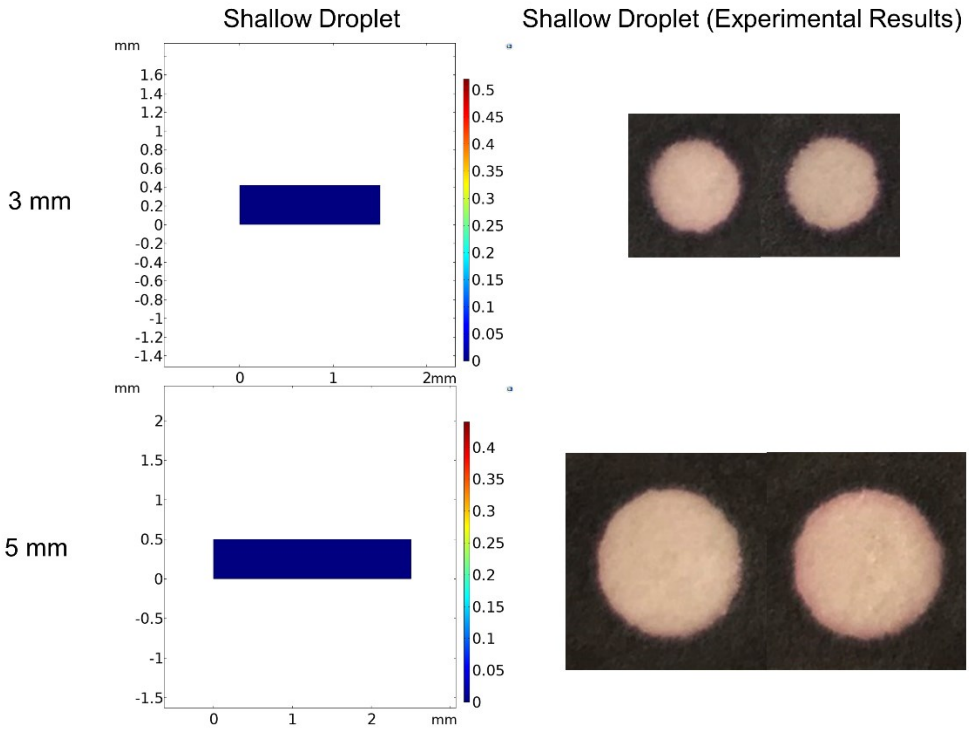

Figure S3: Conversion in 20 µL and 3 µL (3 mm zone)/10 µL (5 mm zone) droplets at 200 s

References

(1) Encinas, M. V.; Rufs, A. M.; Bertolotti, S. G.; Previtali, C. M. Xanthene Dyes/Amine as Photoinitiators of Radical Polymerization: A Comparative and Photochemical Study in Aqueous Medium. *Polymer (Guildf).* **2009**, *50* (13), 2762–2767. https://doi.org/10.1016/j.polymer.2009.04.024.

(2) Kaastrup, K. Photopolymerization-Based Signal Amplification: Mechanistic Characterization and Practical Implementation, Massachusetts Institute of Technology, 2015.

(3) Das, S.; Schuchmann, M. N.; Schuchmann, H. -P; Sonntag, C. Von. The Production of the Superoxide Radical Anion by the OH Radical-induced Oxidation of Trimethylamine in Oxygenated Aqueous Solution. The Kinetics of the Hydrolysis of (Hydroxymethyl)Dimethylamine. *Chem. Ber.* **1987**, *120* (3), 319–323. https://doi.org/10.1002/cber.19871200311.

(4) Beuermann, S.; Paquet, D. A.; McMinn, J. H.; Hutchinson, R. A. Determination of Free-Radical Propagation Rate Coefficients of Butyl, 2-Ethylhexyl, and Dodecyl Acrylates by Pulsed-Laser Polymerization. *Macromolecules* **1996**, *29* (12), 4206–4215. https://doi.org/10.1021/ma960081c.

(5) Stach, M.; Lacík, I.; Chorvát, D.; Buback, M.; Hesse, P.; Hutchinson, R. A.; Tang, L. Propagation Rate Coefficient for Radical Polymerization of N-Vinyl Pyrrolidone in Aqueous Solution Obtained by PLP-SEC. *Macromolecules* **2008**, *41* (14), 5174–5185. https://doi.org/10.1021/ma800354h.

(6) Zwicker, E. F.; Grossweiner, L. I. Transient Measurements of Photochemical Processes in Dyes. II. The Mechanism of the Photosensitized Oxidation of Aqueous Phenol by Eosin. *J. Phys. Chem.* **1963**, *67* (3), 549–555. https://doi.org/10.1021/j100797a004.

(7) Görner, H. Oxygen Uptake Induced by Electron Transfer from Donors to the Triplet State of Methylene Blue and Xanthene Dyes in Air-Saturated Aqueous Solution. *Photochem. Photobiol. Sci.* **2008**, *7* (3), 371–376. https://doi.org/10.1039/b712496a.

(8) Chrysochoos, J. Pulse Radiolysis of Phenylalanine and Tyrosine. *Radiat. Res.* **1968**, *33* (3), 465–479. https://doi.org/10.2307/3572404.

(9) Anseth, K. S.; Wang, C. M.; Bowman, C. N. Kinetic Evidence of Reaction Diffusion during the Polymerization of Multi(Meth)Acrylate Monomers. *Macromolecules* **1994**, *27* (3), 650–655. https://doi.org/10.1021/ma00081a004.

(10) Maillard, B.; Ingold, K. U.; Scaiano, J. C. Rate Constants for the Reactions of Free Radicals with Oxygen in Solution. *J. Am. Chem. Soc.* **1983**, *105* (15), 5095–5099. https://doi.org/10.1021/ja00353a039.

(11) Miller, E. A.; Baniya, S.; Osorio, D.; Jabbour, Y.; Maalouf, A.; Sikes, H. D. Paper-Based Diagnostics in the Antigen-Depletion Regime : High-Density Immobilization of RcSso7d-Cellulose-Binding Domain Fusion Proteins for e Ffi Cient Target Capture. *Biosens.*

Bioelectron. **2018**, *102* (August 2017), 456–463.

(12) Lathwal, S.; Sikes, H. D. Assessment of Colorimetric Amplification Methods in a Paper-Based Immunoassay for Diagnosis of Malaria. *Lab Chip* **2016**, *16* (8), 1374–1382. https://doi.org/10.1039/C6LC00058D.

(13) Yee, E. H.; Lathwal, S.; Shah, P. P.; Sikes, H. D. Detection of Biomarkers of Periodontal Disease in Human Saliva Using Stabilized, Vertical Flow Immunoassays. *ACS Sensors* **2017**, *2*, 1589–1593. https://doi.org/10.1021/acssensors.7b00745.

(14) Nishihara, G. N.; Ackerman, J. D. On the Determination of Mass Transfer in a Concentration Boundary Layer. *Limnol. Oceanogr. Methods* **2007**, *5* (2), 88–96. https://doi.org/10.4319/lom.2007.5.88.